Det Naturvidenskabelige Fakultet
KØBENHAVNS UNIVERSITET

June 15, 2016

Stability analysis of power grid topologies

Lars Reiter Nielsen

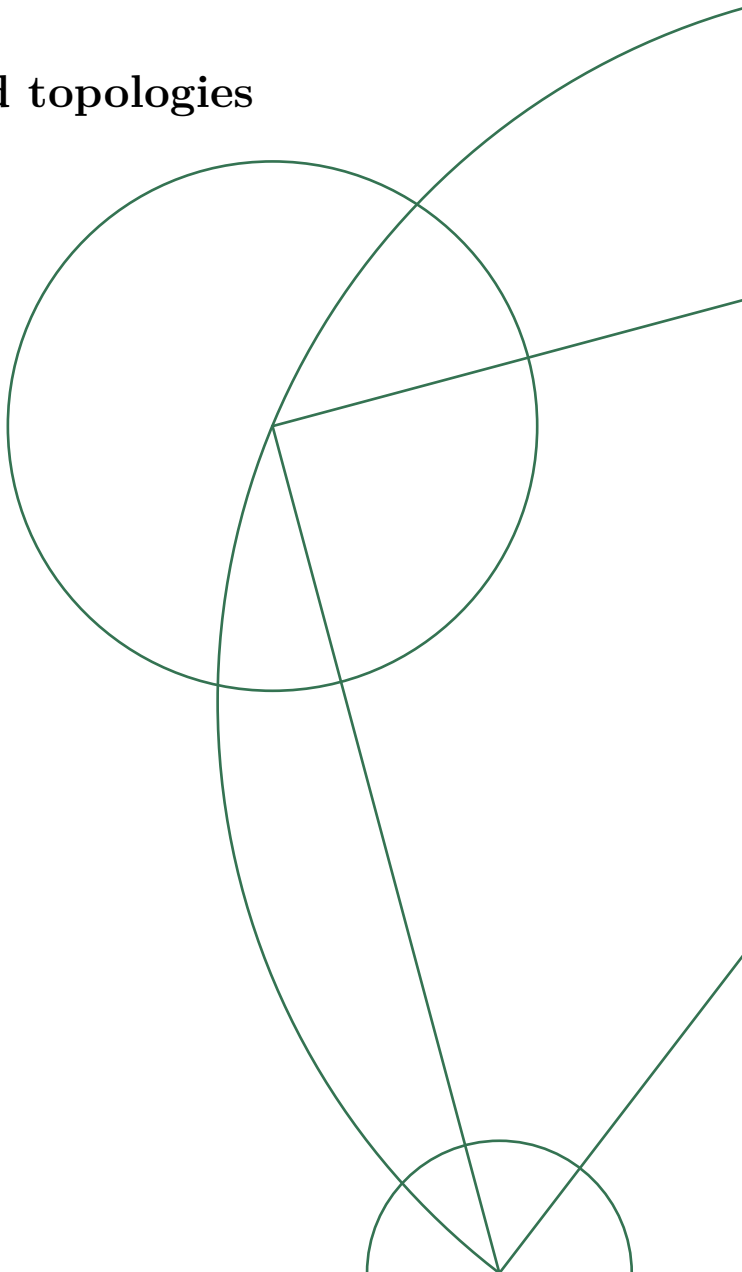

Vejleder: Peter Ditlevsen

Abstract

We use the Kuramato model to answer stability questions of simple and complex power grids. Our motivation to use a physical model stems from the fact that power grids are becoming increasingly complex, due to the advent of multiple minor energy sources. We introduce Braess Paradox as a vital intrinsic (in)stability factor of power grids. Based on data supplied by Energinet.dk, we will investigate structural stability and the presence of Braess Paradox on coarse replications of the danish power grid. We identify the nature of Braess Paradox and show that increased complexity potentially leads to a less robust power grid.

Contents

1 Introduction

1.1 Motivation

For many, the word "energy" is a word generally reserved for physics classes or when discussing the nutrition facts of certain comestibles. Almost as frequently however, the word makes its appearance in the public debate when discussing the need for a green transition, promoting more renewable energy sources that could eventually replace the contemporary solutions, that is taking its toll on the global environment. We are of course talking about large traditional power plants, which burns fossil fuel such as coal and with a high emittance of greenhouse gasses.

Energy sources such as power plants and windmills are all connected to the larger power distribution grids which in Denmark is managed by the company Energinet.dk. The same company published in 2015 their vision for the future power grid [2], which by experts could revolutionise our lives the same way the internet did.

Of particular interest is the predicament of a significant increase in private electricity solutions, such as electric heat pumps, solar panels and our very own miniature power plants. In addition to this, the energy will be primarily supplied by green energy sources such as windmill parks and power plants fuelling biomass.

This all sounds very promising, but with so many new solutions attached to the power grid comes a changing and potentially more complex network, which raises stability questions. Today stability is to some extent centrally controlled (cf. [5, conclusion]), but with many new elaborate private connections not actively controlled, the stability relies more on the physical properties and behaviour of the grid which motivates the use of a physical model.

In this paper we will examine the stability of a couple of simple networks (or "topologies") and ultimately move on to more complex networks replicating a real life power grids. We will introduce non-intuitive stability behaviour described as Braess Paradox and measure its impact on the topologies at hand.

Our model of choice will be inspired by the non-linear Kuramato model [13], describing a system of coupled oscillators. For our purpose, the oscillators represents consumers and generators which is assumed to be synchronous motors (from here, just oscillators). The oscillators are globally coupled and the governing equation (see appendix A for details) reads:

$$\ddot{\phi_j} = P_j - \alpha_j \dot{\phi_j} + \sum_{i=1}^{N} K_{ij} \sin(\theta_j - \theta_i)$$

Here $\theta_j = \Omega t + \phi_j$ is the mechanical phase of oscillator j and Ω is the utility angular frequency of the power grid, ϕ_j is the phase deviation at oscillator j. K_{ij} is the coupling strength between oscillator i and j.

Let us underline that this papers only target is to shed some light on the robustness (or lack thereof) of coarse power grid constructions using a physical model. We hold no illusions that we are able to give a thorough conclusion on stability criteria of future power grids.

1.2 Paper structure

This paper is divided intro three independent analysis. All sections aim to capture information regarding the stability of the networks.

Initially, we will consider a $N = 2$ oscillator topology consisting of one consumer and one generator. With only 2 oscillators, the model takes a particular simple form suitable for a analytical approach. Therefore we will analyse the setup theoretically and subsequently talk about the numerical results. We will try and determine the critical coupling strength K_c at which the oscillators run in synchrony. Then we will check the robustness of the "grid", during a power perturbation.

Next we analyse a $N = 5$ oscillator topology. In this setup, an analytical approach is cumbersome and instead our focus will be on interpreting the numerical results. Under the assumption of a constant coupling strength, we will determine the critical value K_c and then we will see an example of Braess Paradox (discussed in section 2).

With the introduction of Braess Paradox in power grid topologies, we will move on to large $N = 30$ oscillator power grids all with a general frame based on the future power grid found at Energinet.dk (appendix C). Here we will simulate multiple restrictive-random topologies (restrictive, because they have the same "frame" in common) and try to quantify Braess Paradox. We will also try to answer stability questions regarding the structure of the topology.

To start it out, we will give a brief introduction to Braess Paradox and discuss its importance in the context of power grid stability analysis.

2 Braess paradox

The structure of power grids is by no means arbitrary. Beside the practical and economical challenges such as strategic placement of transformer stations and pylons and utility minimization, engineers must also consider that the presumed "optimal" setup could actually be less stable than some other less appealing one.

Naturally one might expect that adding additional lines to an already existing power grid would only increase synchrony, and that adding line capacity (increasing coupling strength) would do no harm either, but in both cases counter examples exists [6] showing that grid stability is a more complex matter.

This non-intuitive behaviour is known as Braess Paradox which has been detected in several systems, but is mostly associated with traffic networks. To get a feeling for Braess Paradox, we will list two short examples that serve to illustrate the paradox (Inspired examples, see [3]).

A star player in sport could reduce the overall performance of the team. In the spirit of football, and considering that the 2016 UEFA European Championsship is kicked off this summer, lets take a quick look at the Portuguese national team. The Portuguese player Christiano Ronaldo is rated as one of the top players in the world, yet the Portuguese national team always fail to make an impact in any international cups, despite the high overall quality of the team. Could it be that the hierarchical structure makes each player more inclined to play Ronaldo, rather than to make the "optimal" decision thus reducing the performance of each of Ronaldos teammates, and would it then promote higher performance if Ronaldo was not in the game, even though he is a star player?

New fast road results in slow moving traffic. Consider exactly two roads combining point A with point B, both with a travel time $T = Ln$ where n is the number of drivers on the road and $L \equiv 2$ is the identical length of each road. Assume that there is N daily drivers taking either the first or the second road, and assume they have no inclination to take either road. We expect that on average there will be $\frac{N}{2}$ drivers taking either road, which amounts to a travel time $T_0 = L\frac{N}{2} = N$. Now assume that a new fast road to B is introduced halfway between point A and B on each road (i.e. the fast road starts a distance $\frac{L}{2} = 1$ between A and B on each road) with a travel time $\frac{3L}{8}n$. Initially there will be no advantage in taking either the first or the second road, so we expect $\frac{N}{2}$ drivers to pick either of the two. Halfway across, the drivers on both roads will reason that taking the fast road IS fastest, because $\frac{3L}{8}\frac{N}{2} < \frac{L}{2}\frac{N}{2}$. But because drivers from both roads merge on the fast road we find a total travel time $T_1 = \frac{L}{2}\frac{N}{2} + \frac{3L}{8}N = \frac{N}{2} + \frac{3}{4}N = \frac{5}{4}N$ and observe that $T_0 < T_1$.

The origin to Braess Paradox is dependent on the system in question, for instance the presence of Braess Paradox in our fast road example can be linked to Nash equilibrium [15]. Nevertheless these examples serve as a warning that connections in the power grid must be chosen with deliberation. For instance, the temptation to relieve a heavily loaded area by adding new lines could have the opposite effect such that the grid is more prone to a complete blackout.

Lets also for a second envision the future grid as predicted by Energinet.dk, which will supposedly feature multiple new minor energy sources attached here and there. This could potentially manifest itself in the most fragile grid we ever had, as there is no saying which links that could give rise to unwanted desynchronization.

We will investigate Braess Paradox in more depth later in this paper.

3 The numerical model

3.1 2N-dimensional vector form

To properly analyse the synchrony and non-synchrony of our coupled oscillator model (the kuramato model), we set up our numerical scheme under a few chosen constructive steps.

Our starting point is the N-oscillator grid model (see appendix A for a rigorous derivation) with the governing equation:

$$\ddot{\phi}_j = P_j - \alpha_j \dot{\phi}_j + \sum_{i=1}^{N} K_{ij} \sin(\theta_i - \theta_j)$$

This is a second order differential equation, and can be reduced to two first order differential equations through the substitution $\omega_j := \dot{\phi}_j$:

$$\dot{\omega}_j = P_j - \alpha_j \omega + \sum_{i=1}^{N} K_{ij} \sin(\theta_i - \theta_j) := f(\omega_j, \theta_j) \tag{1}$$

$$\dot{\phi}_j = \omega_j := g(\omega_j, \theta_j) \tag{2}$$

We now define the state vector $\mathbf{x}_j = (\omega_j, \phi_j)^T$ and the *system* state vector $\mathbf{X} = (\mathbf{x}_1, \mathbf{x}_2, ..., \mathbf{x}_N)^T$. Introducing the function $F : \mathbb{R}^{2N} \to \mathbb{R}^{2N}$ defined as

$$F(\mathbf{X}) = \Big((f(\mathbf{x}_1), g(\mathbf{x}_1))^T, (f(\mathbf{x}_2), g(\mathbf{x}_2))^T, ..., (f(\mathbf{x}_N), g(\mathbf{x}_N))^T \Big)^T$$

we can compare with (1) and (2) to obtain a vector equation for a N-oscillator system in the simple form:

$$\dot{\mathbf{X}} = F(\mathbf{X}) \tag{3}$$

3.2 4th order Runge-Kutta

We will now apply a (4th order) Runge Kutta scheme [8] to our vector form equation (3), hence we define the quantities ("slope estimates"):

$$\mathbf{K}_1 = F(\mathbf{X}) \qquad \mathbf{K}_2 = F(\mathbf{X} + \Delta t/2\mathbf{K}_1) \qquad \mathbf{K}_3 = F(\mathbf{X} + \Delta t/2\mathbf{K}_2) \qquad \mathbf{K}_4 = F(\mathbf{X} + \Delta t\mathbf{K}_3)$$

where Δt is the timestep. We then approximate $F(\mathbf{X})$ with the weighted average:

$$F(\mathbf{X}) = \frac{1}{6}(\mathbf{K}_1 + 2\mathbf{K}_2 + 2\mathbf{K}_3 + \mathbf{K}_4) + O(\Delta t^4) \tag{4}$$

Considering equation (3) again, we will now use the forward euler method with the approximation (4) to arrive at:

$$\mathbf{X}(t + \Delta t) = \mathbf{X}(t) + \frac{\Delta t}{6}(\mathbf{K}_1 + 2\mathbf{K}_2 + 2\mathbf{K}_3 + \mathbf{K}_4) + O(\Delta t^5)$$

The basic idea is that because of the explicit forward euler method, we progress linearly for each timestep Δt:

$$\mathbf{X}(t + \Delta t) = \mathbf{X}(t) + \Delta t F(\mathbf{X})$$

Instead of taking the long shot directly and arrive at $\mathbf{X}(t + \Delta t)$ (which could for all we know be quite off target with respect to the exact solution), we choose a new refined slope $F(\mathbf{X})$ as a weighted average of each estimate slope $\mathbf{K}_1, \mathbf{K}_2, \mathbf{K}_3$ and $\mathbf{K}_4$, choosing the weights which minimizes the truncation error. This ultimately gives us $F(\mathbf{X}) \approx \frac{1}{6}(\mathbf{K}_1 + 2\mathbf{K}_2 + 2\mathbf{K}_3 + \mathbf{K}_4)$. Consider figure 15 for an illustration in two dimensions.

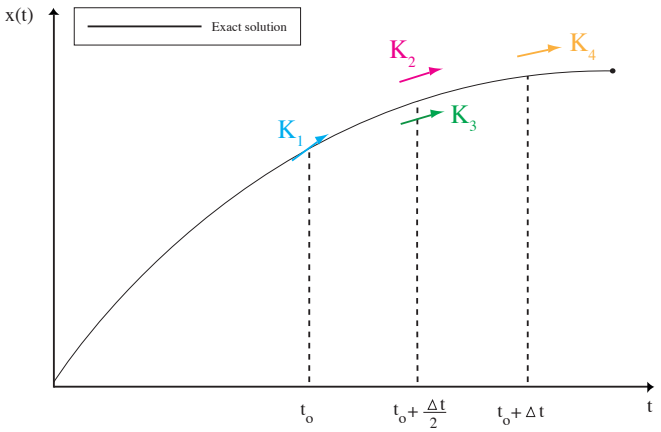

Figure 1: RK4 technique on 2d scale. Arrows symbolize slope estimates at the given position.

3.3 Simulation procedure: Code description and semantics

Let us quickly walk through selected simulation codes used to provide the results of this paper. A link to a downloadable zip file containing *all* relevant scripts can be requested by contacting me on mail: lars.reiter.nielsen@gmail.com

We will use *pseudo*-matlab code to illustrate the procedures. Notice that *not-yet-introduced concepts* such as *critical coupling strength* and *phase order parameter* will appear, therefore it can be fruitful to read this section cursorily and return here following later sections.

For our simulations we make use of three auxiliary functions, namely *CreateAdj*, *findKc* and *NnodeSim*.

CreateAdj description:

1. **Arguments (3):** N (number of oscillators), V (number of edges/links in the topology, M (an optional sparse and symmetric $N \times N$ matrix which restricts the randomization of the output matrix)
2. **Output (1):** 'Random' $N \times N$ connection matrix A with the specified settings. The connection matrix fulfils that $A(i,j) = 1$ if oscillator i and j is connected.
3. **Procedure:**
   (a) Define $A := zeros(N,N)$ ($N \times N$ zero matrix) OR $A := M$ (if M is given as input).
   (b) Loop over each row i in A and check if the entire upper triangular part $A(i,(i+1)...N)$ is empty, if empty add 1 to random column $j = randomInt([i+1,...,N])$, that is $A(i,j) = 1$. Since any adjacency matrix is symmetric, we have now ensured global coupling by defining $A := A + Transpose(A)$.
   (c) If V is a input parameter and $V > N$ we are $V - N$ links short from the specified connection matrix, thus we locate $V - N$ random zero elements in the upper triangle of A and define $A(idx_i) = 1$ where idx_i for $i = 1...(V-N)$ is the index number of a random zero element in the upper triangle.
   (d) If V is NOT an input parameter, we connect a random number of entries (maximum of N), that is $A(idx_i) = 1$ where $idx_i = randomInt([0,1])$ for $i = 1...N$.
4. **Other versions:** *CreateAdj2* is a variant of *CreateAdj* that takes four arguments $N, pmax, V$ and M. The procedures are similar except that a constant coupling strength can now be integrated in the final connection matrix even though an input matrix M is given. In this case only M defines the variable link capacity values. Furthermore, *CreateAdj2* allows the input matrix M to have dimensions less than N, such that M only determines the link properties of oscillator pairs with index less than $\dim(M)$.

NnodeSim description:

1. **Arguments (8):** *time* (simulation runtime), *dt* (timestep size), *alpha* (dissipation factor, assumed constant), A ($N \times N$ connection matrix), $P0$ (N dim power vector with $P0(i)$ being consumed/generated power at oscillator i), $W0$ (N dim ω-vector with $W0(i) \equiv \omega_i(t=0)$), $T0$ (N dim θ-vector with $T0(i) \equiv \theta_i(t=0)$), $idx = [i,j]$ with $i,j \in [1,...,N]$.

2. **Output (5):** $Time$ vector with $\frac{time}{dt}$ entries that collect every time unit of the entire simulation. $TimeR$ vector that collects time units starting halfway into the simulation:

$$TimeR(i) = \frac{time}{2} + i \cdot dt - \frac{time}{2} = i \cdot dt$$

for $i = 1...\frac{time}{2dt}$. $Theta$ vector with

$$Theta(i) = (\theta_1(t = i \cdot dt), ..., \theta_N(t = i \cdot dt))^T$$

for $i = 1...\frac{time}{dt}$. $Power$ vector which contains the transferred power between oscillator $idx(1)$ and $idx(2)$, i.e. $P(i) = K \sin(\theta(idx(1)) - \theta(idx(2)))$ with K being the constant coupling strength. Finally, the function returns the vector R which contains the phase order parameter at times corresponding to $TimeR$.

3. **Procedure:**
   (a) Applies the Runge Kutta Scheme. Defines $X = [W0, T0]$ and defines a sub-function $F(X)$ as described by equation (4).
   (b) For each timestep t we update accordingly: $X = X+F(X)$ and append to $Time$, $Power$ and $Theta$ vector.
   (c) If $t > \frac{time}{2}$ we calculate the (instantaneous) phase order parameter and append to R vector. We also save time t in $TimeR$ vector.
4. **Other versions:** *NnodeSimCritVal* takes the same arguments as *NnodeSim* (except for idx) and returns a single output quantity, namely the *long time average* phase order parameter $Rinf$. The calculations are identical to that of *NnodeSim* except that we calculate $Rinf = \frac{sum(R)}{length(R)}$ at the end of the time loop.

findKc description:

1. **Arguments (7):** Same arguments as for NnodeSim, excluding the last argument idx.
2. **Output (2):** The critical coupling strength Kc and the *long time average* phase order parameter $Rinf$ (see B).
3. **Procedure:**
   (a) Define the maximum and minimum coupling strength that will be considered: $K_{max} = 20$ and $K_{min} = 0$.
   (b) Initialize $K = \frac{K_{max} - K_{min}}{2}$ and set $K_0 := K$ for later use.
   (c) Determine the *long time average* phase order parameter $Rinf$: $NnodeSimCritVal(time, dt, alpha, K \cdot A, P0, W0, T0)$. Notice the use of $K \cdot A$ as the input connection matrix.
   (d) If $Rinf > 0.05$ we conclude that $K = K_{max}$ results in a steady state (B), thus the critical coupling strength Kc must be located in $[K_{min}, K]$. If $Rinf \leq 0.05$ we reason that no steady state exists yet and look for Kc in $[K, K_{max}]$.
   (e) If $Rinf > 0.05$ we set $K_{max} := K$ otherwise if $Rinf \leq 0.05$ we set $K_{min} := K$.
   (f) We repeat step (b) - (e) until $|K_0 - K| < \epsilon$ or if $K < \epsilon$ and $Rinf < 0.05$ in which case no steady state can exist.

Any of the the simulations carried out will use at least one of the above functions. While the scripts are not as readable as they probably should be (due to frequent modifications), hopefully this section can offer some support and limit potential moments of confusion.

Before moving on we will briefly talk about the general procedure at which Braess Paradox is identified (cf. [6]).

Our starting point is a N oscillator topology operating in synchrony. By using the *findKc* procedure we are able to determine the critical coupling strength K_c. To discover Braess Paradox on existing or potential links connecting any pair of oscillators, we will remove or add links respectively. In doing so the system will likely tend to a new steady state.
Within this state we will use the *findKc* procedure once again to determine the new critical coupling strength K_c^{bp}. If by removing a link we find that $K_c^{bp} < K_c$ we will reason that in doing so, we have increased the overall synchrony of the grid and we say that the relevant link induces Braess Paradox. Conversely, if by adding a link we find that $K_c^{bp} > K_c$ the link is also said to induce Braess Paradox.

These observations are put to use in two of our multiple simulations. In the script *SimScript-BraessParadoxNewLinks* we *add* links and try to detect Braess Paradox whereas in *SimSript-BraessParadoxIncComplexity* we *remove* links one at a time.

We also study Braess Paradox by increasing the coupling strength of certain links, this experiment is played out in the script *SimScriptBraessParadoxLinkStr*. The idea here is that we operate our grid at the critical value K_c calculated by *findKc*, which also gives us the *long time average* phase order parameter r_∞ (to be defined). We will then increase link capacity one link at a time, and recalculate the critical coupling strength K_c^{bp} as well as r_∞^{bp}. If either $r_\infty^{bp} \approx 0$ or $K_c^{bp} > K_c$ we obtained a limit cycle or a decrease in synchrony respectively, and will argue that the link is prone to Braess Paradox.

4 One generator and one consumer

Let us now consider the simplest power grid topology, namely one consumer and one generator. We assume equal coupling strength, dissipations factors (a common convention, usually $\alpha = 0.1$ [4] [5] [6]) and also identical moment of inertia of each rotating machine (see appendix A for details.)

The setup is analysed using the grid model and only considering the phase difference, thus the relevant equations becomes:

$$\dot{\Delta\omega} = \Delta P - \alpha\Delta\omega + K\sin(-\Delta\theta) - K\sin(\Delta\theta) = \Delta P - \alpha\Delta\omega - 2K\sin(\Delta\theta) \tag{5}$$

$$\dot{\Delta\theta} = \Delta\omega \tag{6}$$

Where we used that sine is odd, i.e. $\sin(-\Delta\theta) = -\sin(\Delta\theta)$. By inspection we notice two fix points corresponding to:

$$F_1 = \begin{pmatrix}\Delta\omega\\ \Delta\theta\end{pmatrix} = \begin{pmatrix}0\\ \arcsin(\frac{\Delta P}{2K})\end{pmatrix} \qquad F_2 = \begin{pmatrix}\Delta\omega\\ \Delta\theta\end{pmatrix} = \begin{pmatrix}0\\ \arcsin(\pi - \frac{\Delta P}{2K})\end{pmatrix}$$

We would surely argue that F_1 and F_2 only appears if the load is no larger than the link capacity $\Delta P < 2K$. To handle this assertion, we introduce the phase order parameter $re^{i\Psi} := \frac{1}{N}\sum_{j=1}^{N} e^{i\theta_j}$

(see appendix B), which offers a way to quantify the synchrony of the oscillators. In total synchrony we observe that $e^{i\theta_j} = e^{i\theta_k}$ for all combinations $i \neq k$ such that $r = 1$.

However, the magnitude of the phase order parameters only give us an instantaneous insight into the state of the oscillators, so we will prefer to consider the average over a period T which gives us the *long time average* phase order parameter:

$$r_\infty = \lim_{T\to\infty} \lim_{t\to\infty} \frac{1}{t} \int_T^{T+t} re^{i\Psi(t')} dt'$$

Now observe figure 2. Here we have considered three different two node grids, where only the load is varied. For each grid we measure the synchrony over a range of different values of coupling strengths (actually $2K$). The pattern is as expected: When $2K < \Delta P$ the oscillators are out of synch. When $2K = \Delta P$ the oscillators become partially synchronized and the synchronization increases for $2K > \Delta P$. This indicates that our assumption was correct and by defining the *critical* coupling strength K_c as the minimum coupling strength for which synchrony exists, we will quickly write $K_c = \frac{\Delta P}{2K}$.

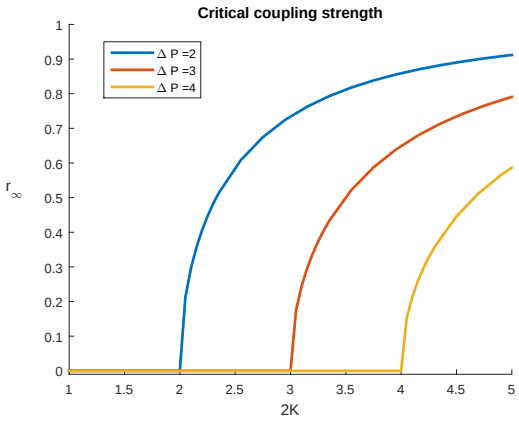

Figure 2: Parameters: Runtime = 1500, $\alpha = 0.1$ and $\Delta\omega_0 = \Delta\theta_0 = 0$

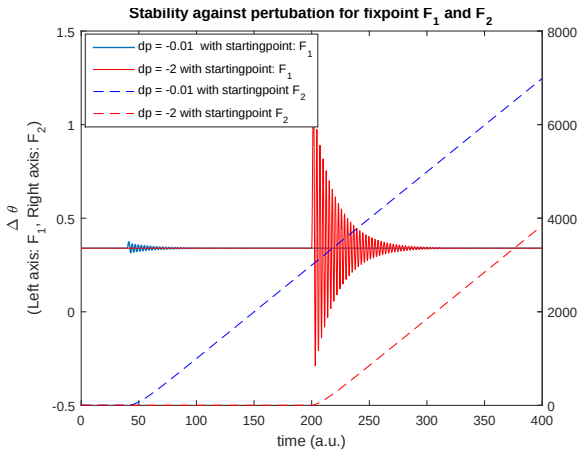

Figure 3: Parameters: Runtime = 500, $\alpha = 0.1$, $\Delta P = 2$, pertubation time duration = 2 units and $(\Delta\theta_0, \Delta\omega_0)^T = F_1$ for solid lines (left-axis) and $(\Delta\theta_0, \Delta\omega_0)^T = F_2$ for dashed lines (right-axis)

A priori we would expect both fix points F_1 and F_2 to be equally stable in the sense that fluctuations in power demand will cause the same system response at either point, but figure 3 shows otherwise. Here we consider two initially synchronized topologies. One topology is running at normal operation at the fix point F_1, while the other is operating at the fix point F_2. We then perturb both systems by increasing the consumer demand with $dP = -0.01$ units of power (red lines; F_1 solid, F_2 dashed) and notice the break of synchrony for the topology operating at the fix point F_2. During a new simulation we perturb the systems with $dP = -2$ (blue lines) and once again notice the break of synchrony of the topology operating at F_2 while the other returns to normal operation. This indicates that F_2 is in fact unstable and breaks down for even small perturbations, while F_1 is a (robust) stable point.

If we focus our attention at the fix point F_1, we will see that at this stable point even large perturbations will not result in a limit cycle (see figure 4) even though the power demand is much higher than the power that is ordinarily fed into the system by the generator. When this

occurs, the missing supply comes from the rotational kinetic energy stored in the generator [5]. There is obviously a limit - both with respect to the duration and magnitude of the perturbation - as to how much the system can cope with before a breakdown. In figure 5 we increased the consumer demand with an additional 0.1 power unit, and we observe that the system does not return to normal operation.

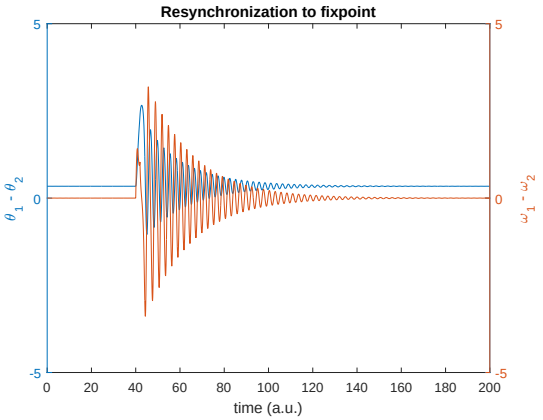

Figure 4: Parameters: Runtime $= 200$, $\alpha = 0.1$, $\Delta P = 2$, pertubation size $dP = -3.3$ and $(\Delta\omega_0, \Delta\theta_0)^T = F_1$

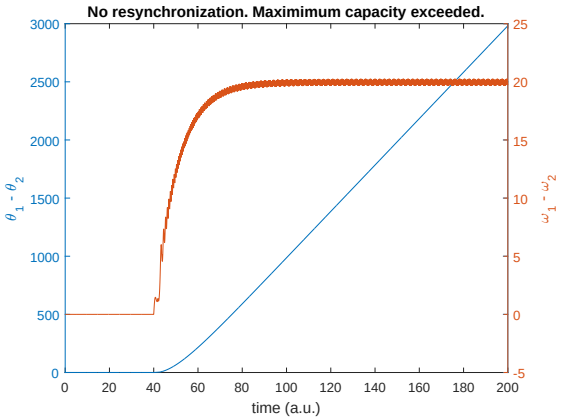

Figure 5: Parameters: Runtime $= 200$, $\alpha = 0.1$, $\Delta P = 2$, pertubation size $dP = -3.4$ and $(\Delta\omega_0, \Delta\theta_0)^T = F_1$

5 Evoking braess paradox

In this section we will dig deeper into the (in)stability properties of power grids by revealing the presence of Braess Paradox as previously described in section 2 on a concrete 5-node power grid. Our grid is made up of three generators and two consumers. One of the generators supply 2 units of power, while the remaining two supply a single unit of power. The two consumers consume an equivalent of 4 units of power (2 units each). The topology is visualized in figure 6.

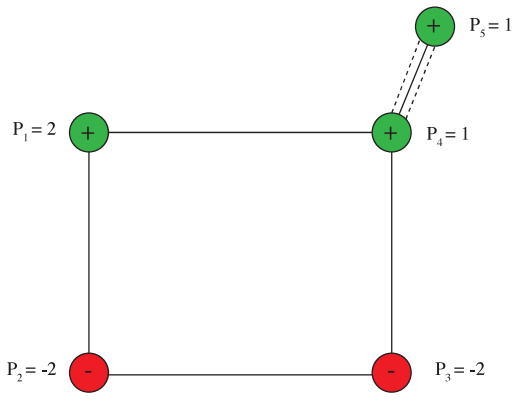

Figure 6: 3 generators (green circles), 2 consumers (red circles). Braess Paradox identified on upper connection.

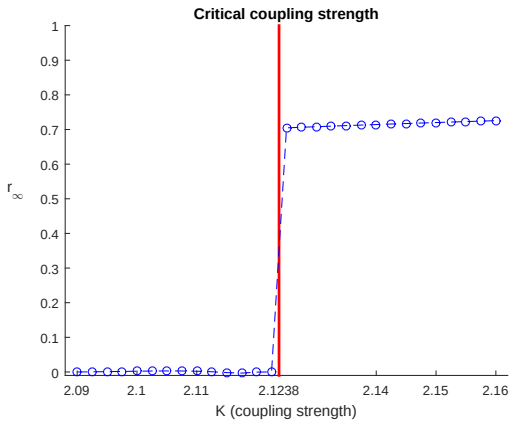

Figure 7: Parameters: $\alpha = 1$, total time $= 400$ a.u. and $\mathbf{X_0} = \mathbf{0}$

We will assume equal coupling strength and dissipation parameters, which in this concrete topology is taken to be $\alpha = 1$. Our first goal is to determine the critical coupling strength K_c, thus we plot the *long time average* phase order parameter r_∞ up against potential capacity values in the range $[2.09, 2.16]$. Our search leads us to a candidate value $K_c \approx 2.13$ as can be seen in figure 7. Let us add that $\mathbf{X_0} = \mathbf{0}$ expresses that $(\theta_i(t=0), \omega_i(t=0))^T = \mathbf{0}$ for $i = 1, 2, 3, 4, 5$. This convention will be carried on to later sections.

Having found a critical value K_c, we run our simulation with $K_{i,j} \equiv K := K_c$ and observe in figure 8 how the 5 oscillators run in synchrony, corresponding to a steady state. With this setup we are on the edge of synchrony, but we would expect that increased capacity would not jeopardize the normal operation of the grid. However, by adding one extra unit of capacity to the link between the upper generators (see figure 6) such that the new coupling strength between this section of the grid is now $K_{3,4} = K_{4,3} = 3.13$ we obtain figure 9 which shows that the decision to increase capacity has resulted in a limit cycle.

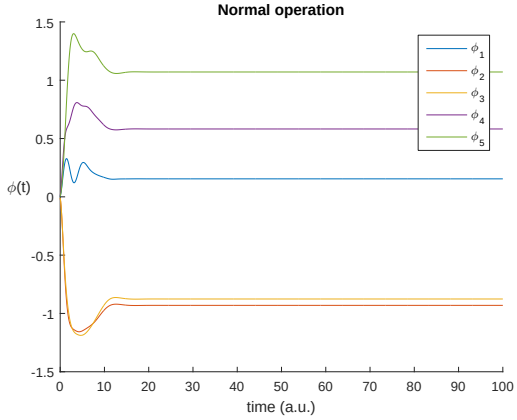

Figure 8: Parameters: $K = 2.13$, $\alpha = 1$ and $\mathbf{X_0} = \mathbf{0}$

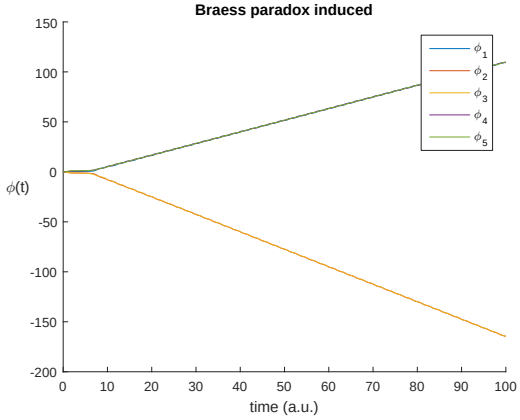

Figure 9: Parameters: $K = 2.13$, $\alpha = 1$, $\mathbf{X_0} = \mathbf{0}$ and $K_{4,5}$ increased

By adding capacity to the upper link, the flow redistribute in such a way that no steady state can exist. Studies show that Braess Paradox in the context of power grid stability can be ascribed to the phenomena known as "Geometric Frustration" [15] [6] where the cyclic sum of the phase differences between each consecutive oscillator pair does not add up to a multiple of 2π such that the phases are not well-defined.

The frequency at which Braess Paradox manifests itself in larger power grids is analysed in the following section.

6 N-node topology

6.1 The future power grid

Up until now we have considered a couple of simple networks, and it is now time to explore larger and more realistic acquaintances. To motivate the upcoming experiment, let us recall that Energinet.dk who manages the highvoltage ($\sim$ 400 kV) and mediumvoltage ($\sim$ 150 kV) distribution grids ([11]) has announced the coming of a new revolutionary smart grid ([2]) which promotes a more flexible and green way to exploit energy.

Within their vision is the prediction of a major advancement in the use of private electricity solutions as well as renewable energy sources, which inevitable results in a complex multi-link power grid.

To get some insight into the stability behaviour of this future power grid, we will simulate different large ($N = 30$) topologies and investigate structural stability criteria. We will then simulate (coarse) real-life topologies with a main structure based on the network map publicly available at Energinet.dk (see [12] or appendix C) but restricting ourselves to the western region (i.e. excluding "Sjælland" and "Bornholm"). See figure 10 for an illustration and compare with appendix C. We will name these 'real-life' topologies as **restrictive** random topologies, whereas the others will be denoted **fully** random topologies.

We will be particular interested in trying to determine and quantify the frequency at which Braess Paradox appears on the replication of the danish grids, that is the **restrictive** random topologies.

6.2 Danish grid structure and model formality

Ordinarily, different lines run at different voltage levels. As such, varying lines are connected by transformer stations which adjust the voltage. For the sake of uniformity and to avoid repeatedly line-to-line load conversions, we will make use of the dimensionless units called per units (p.u.) (see [14], [5, p. 486, top]).

The general idea is that we choose a base voltage level V_b and measure the voltage of each line $V_{i,j}$ as a fraction of the base voltage. i.e. $V_{i,j}^{p.u.} = \frac{V_{i,j}}{V_b}$. By picking out one more quantity - typically power - and convert it to per unit in a similar fashion, we have guaranteed a complete set of dimensionless quantities (cf. [14, base quantities]) and by finally scaling every line-specific load to the same normalized voltage level we can completely omit the integration of transformers in our network (cf. appendix C, red dots). As a result, line coupling strength will be measured w.r.t. the normalized voltage level.

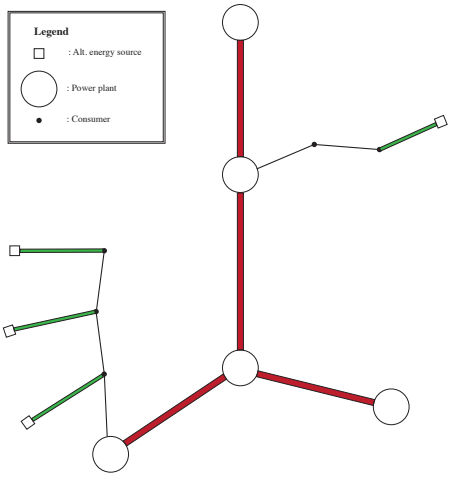

Figure 10: Coarse power grid replication of the westernmost danish grid. Forms the basis of the restrictive-random topologies.

The coloured lines on figure 10 symbolizes different capacity levels. The red lines denote links with a maximum capacity of $K_{i,j} = 7.5$ p.u. Green lines denote links with a maximum capacity of $K_{i,j} = 5$ p.u. and the remainder (black lines) with a capacity of $K_{i,j} = 3$ p.u.

Notice that the danish frame (figure 10) is made up of a total of 14 oscillators (counting generators and consumers). For our simulations, we set the number of oscillators to the fixed value $N = 30$ both for the **fully** and **restrictive** random topologies. This implies that any **restrictive** random topologies 'only' connects $N - 14 = 16$ oscillators into the fixed danish frame, whereas **fully** random topologies randomly connects a total of N oscillators. Notice also

that any randomly connected line on the **restrictive** random topologies will contain a constant capacity of $K_{i,j} = 3$ p.u.

At the beginning of our simulation, we ensure that the grid is in a state of equilibrium such that the total power consumed and the total power generated adds up to zero. The consumed power P_c of each consumer is taken to be the total generated power divided by the number of consumers.

Referring to the data at Energinet.dk ([12]) (and the assumption that energy is mainly generated by renewable sources) we set the total generated power from power plants to $P_{pp} = 9$ p.u. and the total generated power from alternative sources to $P_{alt} = 12$ p.u. such that the generated power at each of the 21 consumer entities equals $P_c = \frac{P_{pp}+P_{alt}}{21} = 1$.

6.3 Complex grid stability analysis

Let us initially cement some basic stability results related to the structure of **fully random** $N = 30$ node topologies.
Consider figure 11 where we for each fixed value of the critical coupling strength K (plotname: P^{max}) simulated 20 topologies and averaged over the set of the respective phase order parameters. The plot illustrates that there is not a general critical coupling strength ($K_c \equiv P_c^{max}$) that is decisive for the stability of an arbitrary N (in this case $N = 30$) node topology, since the average phase order parameter is not stabilizing near 1 as a function of $K \equiv P^{max}$.
In other words, the critical coupling strength leading to normal operation is highly dependent on the structure of the topology, as we might expect.

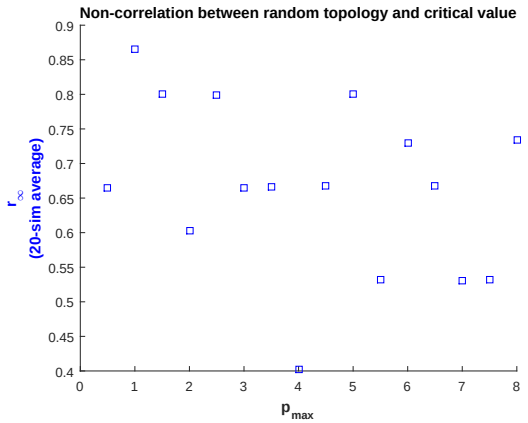

Figure 11: Parameters: $N = 30$, $\alpha = 0.1$, Runtime = 400 a.u. and $\mathbf{X}_0 = \mathbf{0}$

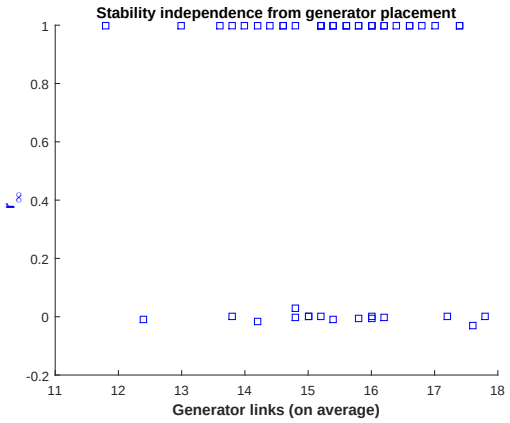

Figure 12: 50 random topologies. Parameters: $N = 30$,$K_c = 10$ $\alpha = 0.1$, Runtime = 400 a.u. and $\mathbf{X}_0 = \mathbf{0}$

On figure 12 we simulated 50 **fully random** grid topologies (be advised that some points overlap), where we varied the *average* number of links protruding from each generator. The figure suggests, that even for a variable number of generator links the systems have roughly the same probability of being in either a steady state or a non-synchronous state, thus there is no apparent connection between stability and the number of links that connect generators with consumers. But this is no general conclusion.
Even though on average the number of links seem to have no impact on the overall stability, studies show that the removal and attachment of specific links could in fact provoke Braess

Paradox, potentially leading to a power outage [6]. This will be the subject when we now turn our attention towards the **restrictive-random** topologies below.

We wish to study the frequency at which Braess Paradox appears on random topologies restricted to the rough frame of the danish distribution grid (figure 10). As previously stated, adding new connection lines can lead to Braess Paradox, but we have also seen in section 5 that Braess Paradox can be induced by increasing link capacity.

For this reason we have simulated a total of 85 **restrictive random** topologies with a random number (ranging from 45 to 60) of arbitrarily placed connection lines. Each of these topologies constitutes the initial setup for our repeated experiment.

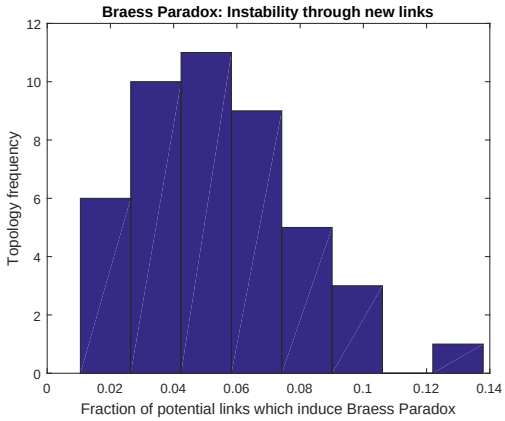

Figure 13: 45 **restrictive random** topologies simulated, parameters: $N = 30$, $\alpha = 0.1$, runtime = 400a.u. and $\mathbf{X} = \mathbf{0}$

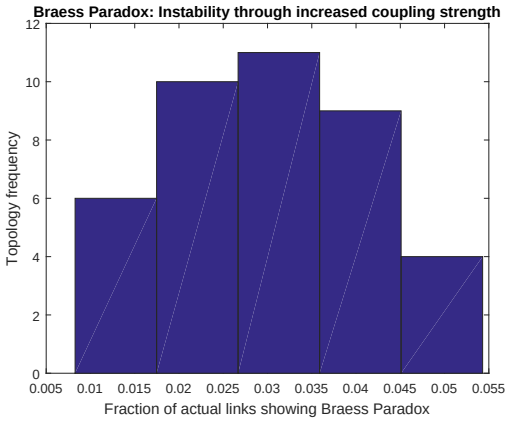

Figure 14: 40 **restrictive random** topologies simulated. Parameters: $N = 30$, $\alpha = 0.1$, runtime = 400 a.u. and $\mathbf{X} = \mathbf{0}$

On figure 13 we examined 40 of the 85 simulated topologies, where the goal was to spot Braess Paradox on potential new links. We identified any potential links (non-existing links) and calculated the critical coupling strength K_c. Next, we 'activated' the set of potential links, one at a time, and recalculated the critical coupling strength K_c^{bp}. If $K_c^{bp} > K_c$ we concluded that the link is prone to Braess Paradox.

For the remaining 45 randomized grids, we measured the fraction of links showing Braess Paradox as depicted in figure 14. For each topology we ensured the existence of a steady state and calculated the critical coupling strength K_c. We then increased capacity of each link, one link at a time, and recalculated the critical coupling strength K_c^{bp} as well as the phase order parameter. If either the steady state was lost or $K_c < K_c^{bp}$ we ascribed it to Braess Paradox.

The procedure of identifying Braess Paradox is also described in section 3.3.

Both histograms (figure 13 and figure 14) indicates that Braess Paradox is in general appearing on less than one out of ten existing and potential links, if we choose to neglect the outlier on figure 13. This is in agreement with other studies on the area (cf. [6, app.C]) that suggests the same low frequency. In particular we see that the probability for Braess Paradox to appear on any arbitrary existing or newly attached link is limited, but increasing the number of links will surely substantiate the appearance of Braess Paradox and potentially destabilize the power grid.

Furthermore, figure 14 suggests the following expected value $E_{BP}^{ActiveLinks} \approx 3\%$ (the average

number of existing links prone to Braess Paradox) while figure 13 features the following approximate expectation $E_{BP}^{NewLinks} \approx 5\%$ (the average number of potential links prone to Braess Paradox). In conclusion, our multiple randomized replications of the (westernmost) Danish power grid indicates a weak presence ($E_{BP}^{NewLinks} \approx 5\%$) of Braess Paradox on new potential links, while the tendency is slightly lower ($E_{BP}^{ActiveLinks} \approx 3\%$) on already existing links.

7 Discussion

Decentralized power grids will be a likely future outcome, following the introduction of the evolutionary smartgrid [2]. The highly articulated local distribution grids will presumable be able to accommodate regional consumer demand, making active control obsolete.

The emerging complex power grid can effectively be analysed on the basis of a physical model as we demonstrated throughout this paper. With less active control, the dynamics and stability of the network relies more on the structure and properties of the grid and as such accounting for network stability criteria is vital. We have been acquainted with Braess Paradox, and seen that while Braess Paradox is in general elusive and infrequent on new links as well as existing ones, the high increase in new energy sources attached to the grid will substantiate the possibility for fatal stability issues and potential blackouts.

We found that coarse replications of the future Danish power grid showed the possibility of Braess Paradox on an average of 3% of existing links and 5% of potential new links, which offers a quiet warning that increased complexity begs for increased monitoring.

8 Acknowledgements

This project is inspired by existing papers on the subject, in particular "Analysis of a power grid using a Kuramato-like model"[5] and "Braess's paradox in oscillator networks, desynchronization and power outage"[6].

A special thanks to Peter Ditlevsen for introducing me to this exciting subject and for his support throughout the weeks. Especially at the upstart, our conversations gave me a much wider understanding of the technicalities concerning the power grid mechanics. During the programming period, Peter also offered his assistance in trying to clarify the validity of simulation results.

Also a thanks to Jakob Guldberg Aaes for supplying the front page LaTeX package and to Mia Phillippa Nørlund Fabricius for the creation of all the graphical illustrations.

A Deriving the grid model

Consider a power grid consisting of N oscillators (rotating machines). Each oscillator represents a generator or consumer. The power grid usually runs at a utility frequency of 50 Hz, which gives us a utility *angular* frequency of $\Omega = 2\pi \times 50$ Hz. The frequency could also be taken as 60 Hz depending on the power grid in question.

If we consider an arbitrary oscillator j and let $\phi_j(t)$ denote the deviation from the net frequency, we can write the mechanical phase as:

$$\theta_j(t) = \Omega t + \phi_j(t)$$

For any oscillator j, we can use the law of energy conservation to determine the consumed or generated power:

$$P_j^{oscil} = P_j^{acc} + P_j^{diss} + \sum_{i=1}^{N} P_{ij}^{trans}$$

Here P_j^{oscil} is the power at oscillator j, $P_j^{acc} = \frac{1}{2} I_j \frac{d}{dt}(\dot{\theta}_j)^2 = I_j \ddot{\theta}_j \dot{\theta}_j$ is the rate at which kinetic rotational energy is accumulated in the machine, $P_{ij}^{diss} = \kappa_j(\dot{\theta}_j)^2$ is the rate of energy dissipation due to friction and finally $P_{ij}^{trans} = P_{ij}^{max} \sin(\theta_i - \theta_j)$ denotes the rate at which energy is surging from oscillator i to oscillator j.

Notice the crude assumption that energy dissipation is only due to friction, ignoring ohmic loss etc.

Inserting the relevant quantities we obtain:

$$\begin{aligned}
P_j^{oscil} &= I_j \ddot{\theta}_j \dot{\theta}_j + \kappa_j(\dot{\theta}_j)^2 + \sum_{i=1}^{N} P_{ij}^{max} \sin(\theta_i - \theta_j) \\
&= I_j \ddot{\phi}_j(\Omega + \dot{\phi}_j) + \kappa_j(\Omega + \dot{\phi}_j)^2 + \sum_{i=1}^{N} P_{ij}^{max} \sin(\theta_i - \theta_j) \\
&= I_j \Omega \ddot{\phi}_j + I_j \ddot{\phi}_j \dot{\phi}_j + 2\kappa_j \Omega \dot{\phi}_j + \kappa_j \dot{\phi}_j{}^2 + \kappa_j \Omega^2 + \sum_{i=1}^{N} P_{ij}^{max} \sin(\theta_i - \theta_j) \\
&:= f(\dot{\phi}_j)
\end{aligned} \tag{7}$$

Under the assumption that each oscillator operates close to the utility frequency ($\dot{\phi}_j \ll \Omega$) we obtain the following 1st order approximation:

$$\begin{aligned}
f(\dot{\phi}_j) &\approx (I_j \Omega \ddot{\phi}_j + \kappa_j \Omega^2 + \sum_{i=1}^{N} P_{ij}^{max} \sin(\theta_i - \theta_j)) + (I_j \ddot{\phi}_j + 2\kappa_j \Omega)\dot{\phi}_j \\
&\approx I_j \Omega \ddot{\phi}_j + \kappa_j \Omega^2 + 2\kappa_j \Omega \dot{\phi}_j + \sum_{i=1}^{N} P_{ij}^{max} \sin(\theta_i - \theta_j)
\end{aligned}$$

In the last line we used that the rate at which kinetic energy accumulates is significantly lower than the rate at which energy dissipate ($I\Omega\ddot{\phi} \ll \kappa\Omega^2$), which is a sensible assumption for mechanical systems (see [5, sec.2, eq. (11)]).

Comparing the approximation with (7) and omitting the weak inequality sign we obtain:

$$P_j^{oscil} = I_j \Omega \ddot{\phi_j} + \kappa_j \Omega^2 + 2\kappa_j \Omega \dot{\phi_j} + \sum_{i=1}^{N} P_{ij}^{max} \sin(\theta_i - \theta_j) \tag{8}$$

Dividing through by $I\Omega$ and defining the new standard variables $P_j = \frac{P_j^{oscil} - \kappa_j \Omega^2}{I_j \Omega}$, $\alpha_j = 2\kappa_j \Omega$, $K_{ij} = \frac{P_{ij}^{max}}{I_j \Omega}$ we can rearrange (8) and recognize the leading equation of the kuramato-like model (cf. [13]):

$$\ddot{\phi_j} = P_j - \alpha_j \dot{\phi_j} + \sum_{i=1}^{N} K_{ij} \sin(\theta_j - \theta_i)$$

From the final equation, we observe that the dynamics of the system depends not on the phases θ_j but only on their deviation from the utility frequency and their mutual difference.

There are a number of natural steps which reduces the complexity of the model. For example. it can be fruitful to assume that the moment of inertia of each rotational machine is identical ($I = I_j$ for all j). Furthermore we might assume that each machine have identically dissipation parameters ($\alpha = \alpha_j$ for all j), in particular we assume that generators and consumers are equally inefficient (!). And last but not least, we might assume that all oscillators are connected with same coupling strength ($K = K_{ij}$ for all i,j).

B Phase order parameter

In order to measure synchrony of an arbitrary grid topology we consider the phase order parameter:

$$re^{i\Psi} := \frac{1}{N}\sum_{j=1}^{N} e^{i\theta_j}$$

where i is the imaginary unit and N the number of oscillators.

Notice that $(\Psi, r) \mapsto r\exp(i\Psi)$ is a mapping into complex space with the property that $r = 1$ if and only if for all j there exist a $k \in \mathbb{N}_0$ such that $\Psi = \theta_j + 2k\pi$, corresponding to full synchrony. Thus the magnitude of the order parameter quantifies the phase-coherence of the oscillators, ranging from zero to one.

As a way of visualizing synchrony, we might choose to make a vector plot of the phase order parameter alongside each $\exp(i\theta_j)$ term. Obviously, the phase-specific terms will traverse the unit circle, whereas the phase order parameter will traverse a circle with a radius less than or equal to 1. See the figure below.

The phase order parameter gives an instantaneous picture of the phase coherence, but it's more relevant to investigate whether or not the oscillators tend to a synchronous state during a period T. For this purpose we define the average phase order parameter [4]:

$$r_\infty = \lim_{T\to\infty}\lim_{t\to\infty}\frac{1}{t}\int_T^{T+t} re^{i\Psi(t')}dt'$$

This is a measure of the average phase coherence in the long time limit, picking out several phase order parameters and taking the average when the system is expected to be stable.

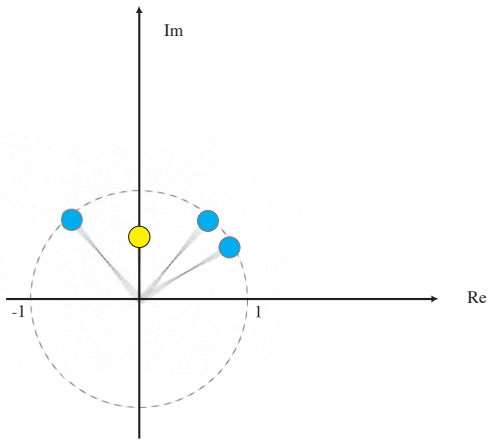

Figure 15: Phase order parameter (yellow circle) for 3-oscillator grid (blue circles)

C Map of the future danish power grid (anno 2020)

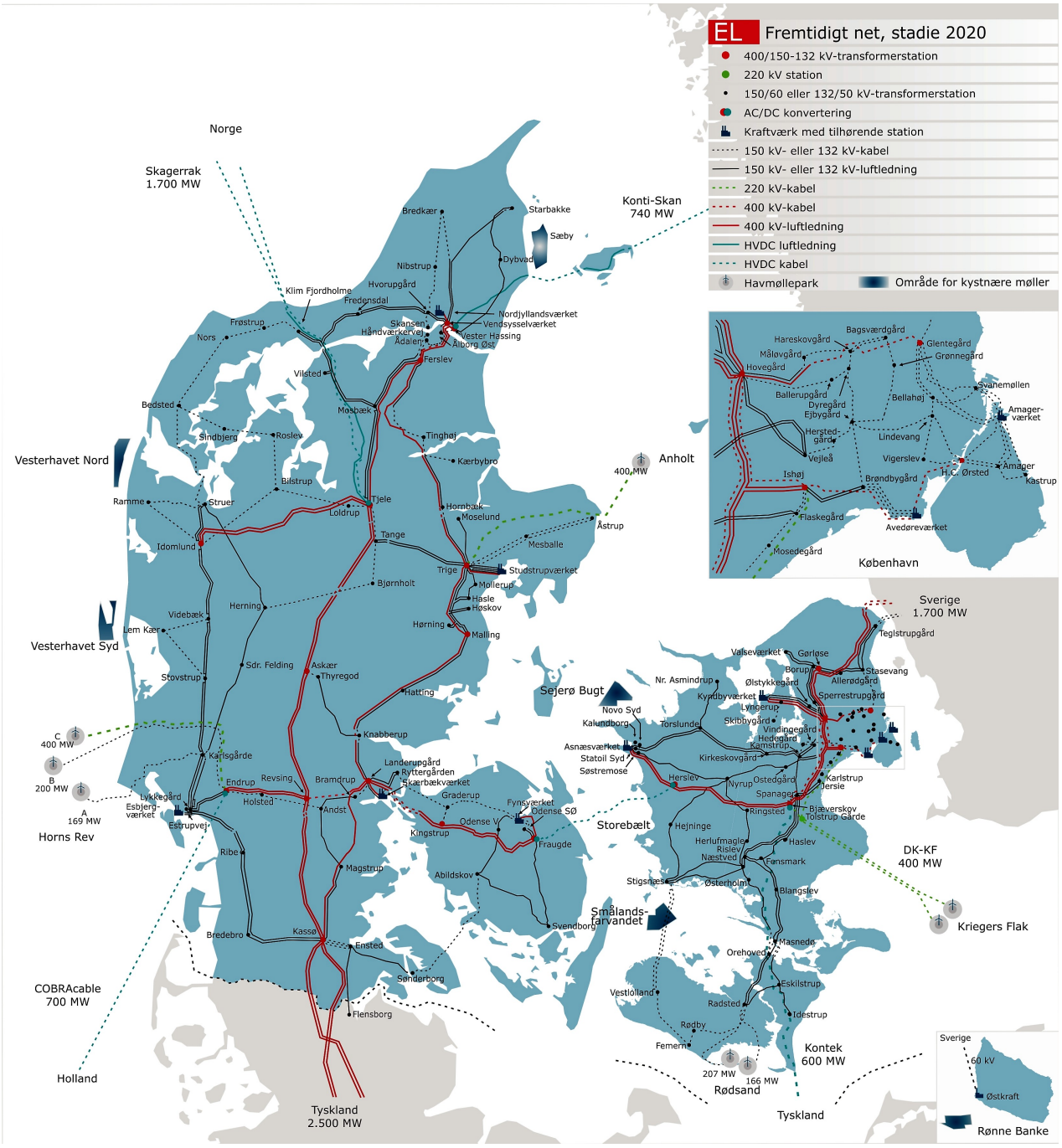

Figure 16: Future danish power grid provided by Energinet.dk

References

[1] Energinet.dk: det danske transmissionsnet, http://energinet.dk/DA/El/Nyheder/Sider/Nu-kan-du-downloade-data-om-det-danske-elsystem-i-2020.aspx, retrieved 14-05-2016

[2] Energinet.dk: fremtidens smartgrid, http://www.energinet.dk/DA/FORSKNING/Energinet-dks-forskning-og-udvikling/Projekter/Sider/Film-Smart-Grid-Danmark.aspx, retrieved 14-05-2016

[3] Wikipedia, The free Encyclopedia: Braess Paradox, https://en.wikipedia.org/wiki/Braess_paradox, retrieved 24-04-2016

[4] M. Rohden, A. Sorge, D. Witthaut and M. Timme. (2014). Impact of network topology on synchrony of oscillatory power grids. Chaos. 2014 Mar;24(1):013123. DOI: 10.1063/1.4865895.

[5] G. Filatrelia, A.H. Nielsen and N.F. Pedersen. (2008). Analysis of a power grid using a kuramato-like model. Eur. Phys. J. B 61, 485–491. DOI: 10.1140/epjb/e2008-00098-8

[6] Dirk Witthaut and Marc Timme 2012 New J. Phys. 14 083036. DOI: https:10.1088/1367-2630/14/8/083036

[7] M. Rohden, A. Sorge, D. Witthaut and M.Timme. (2012). Self-organized synchronization in Decentralized Power Grids. Physical Review Letters 109(6):064101. DOI: 10.1103/PhysRevLett.109.064101

[8] W. Press, B. Flannery, S. Teukolsky and W. Vetterling. (1993). Numerical recipes in FORTRAN 77: The art of scientific computing. Mathematics of Computation 1(205):394,425. DOI: 10.2307/2153422

[9] Energinet.dk: mikrokraftvarme anlæg, http://www.energinet.dk/DA/GAS/Udvikling-af-gasteknologier/Nye-gasforbrugsteknologier/Sider/Mikrokraftvarme.aspx, retrieved 15-05-2016

[10] Sparenergi.dk: private energiløsninger, http://sparenergi.dk/forbruger/el, retrieved 15-05-2016

[11] Energinet.dk: elnet distribution, http://www.energinet.dk/da/anlaeg-og-projekter/generelt-om-elanlaeg/Sider/default.aspx, retrieved 15-05-2016

[12] Energinet.dk: Elsystemet, http://energinet.dk/DA/El/Nyheder/Sider/Nu-kan-du-downloade-data-om-det-danske-elsystem-i-2020.aspx, retrieved 16-05-2016

[13] Wikipedia, The free Encyclopedia: The Kuramato Model, https://en.wikipedia.org/wiki/Kuramoto_model, retrieved 12-05-2016

[14] Wikipedia, The free Encyclopedia: Per-Unit system, https://en.wikipedia.org/wiki/Per-unit_system, retrieved 18-05-2016

[15] Power grid upgrades may cause blackouts, warns Braess's paradox, http://phys.org/news/2012-10-power-grid-blackouts-braess-paradox.html, retrieved 24-05-2016